chemistry proceedings

MDPI

Proceeding Paper

Molecular Docking/Dynamic Simulations and ADME-TOX-Based Analysis of Phthalimido-1,3-Thiazole Derivatives as BCR-ABL Inhibitors †

Imane Bensahbane [1,*], Nadjib Melkemi [1], Ismail Daoud [2,3] and Asli Faiza [1]

[1] Group of Computational and Medicinal Chemistry, LMCE Laboratory, University Mohamed Khider, Biskra 07000, Algeria; n.melkemi@univ-biskra.dz (N.M.); faiza.asli@univ-biskra.dz (A.F.)
[2] Department of Chemistry, Faculty of Sciences, University of Mohamed Khider Biskra, Biskra 07000, Algeria; i.daoud@univ-biskra.dz
[3] Laboratory of Natural Substances and Bioactive (LASNABIO), University of Abou-Bakr Belkaid, Tlemcen 13000, Algeria
* Correspondence: imane.bensahbane@univ-biskra.dz
† Presented at the 29th International Electronic Conference on Synthetic Organic Chemistry (ECSOC-29); Available online: https://sciforum.net/event/ecsoc-29.

Abstract

Acute lymphoblastic leukemia (ALL) is the most common cancer in childhood. 30–50% of its cases are caused by the BCR-ABL1 fusion gene as a driver oncogene. In this research work, a study of the cytotoxic properties of phthalimido-1,3-thiazole derivatives against the BCR-ABL protein PDB ID: 4WA9 was carried out using a combination of different computational chemistry methods, including a molecular docking/dynamics study and ADM-T evaluation. Six top hits were identified based on their free energy scores, namely 4WA9-L21, 4WA9-L20, 4WA9-L22, 4WA9-L19, 4WA9-L18 and 4WA9-L18, which demonstrated better binding affinity (from −8.36 to −9.29 kcal/mol). Furthermore, MD studies support the molecular docking results and validate the stability of the studied complexes under physiological conditions. These results confirm that the hits selected are verifiable inhibitors of the BCR-ABL protein, implying a good correlation between in silico and in vitro studies. Moreover, in silico ADME-TOX studies were used to predict the pharmacokinetic, pharmacodynamics, and toxicological properties of the studied hits. These findings support the future role of phthalimido-1,3-thiazole derivatives against the ALL disease and may help to find a new therapeutic combination of drugs to treat relapsed acute lymphoblastic leukemia and improve overall survival.

Keywords: Ph+ ALL; BCR-ABL; molecular docking; dynamic simulations; ADME-T

Academic Editor(s): Name

Published: date

Citation: Bensahbane, I.; Melkemi, N.; Daoud, I.; Faiza, A. Molecular Docking/Dynamic Simulations and ADME-TOX-Based Analysis of Phthalimido-1,3-Thiazole Derivatives as BCR-ABL Inhibitors. *Chem. Proc.* **2025**, *volume number*, x. https://doi.org/10.3390/xxxxx

1. Introduction

Acute lymphoblastic leukemia (ALL) is the most common cancer in childhood [1]. 30–50% of its cases are caused by the BCR-ABL1 fusion gene as a driver oncogene [2]. The translocation between the BCR gene region on chromosome 9 and the ABL proto-oncogene 1 (ABL1) gene on chromosome 22 promotes the development of Philadelphia Chromosome-Positive Leukemia [3]. The ABL1 kinase domain has recently garnered significant attention as a promising molecular target for the development of Philadelphia chromosome-positive acute lymphoblastic leukemia (Ph+ ALL) treatment Patients with

acute lymphoblastic leukemia suffered from drug resistance. Although there are ABL1 kinase inhibitors with remarkable efficacy, this did not prevent the relapse and resistance of treatments for this cancer; this even itself remains an ongoing challenge [4]. To this end, a recently synthesized series of phthalimido-1,3-thiazole derivatives [5] were collected to predict their cytotoxic properties against the ABL1 kinase domain using different computational chemistry methods such as molecular docking, MD simulation, and in silico ADME-TOX evaluation in order to contribute to the development of new (Ph+ ALL) inhibitors.

Proteins' ability to interact with small molecules plays a crucial role in shaping the dynamics of proteins and therefore impacting their biological functions [6]. Molecular docking was employed for the purpose of predicting the interactions between the ABL1 kinase domain and the studied small molecules. Furthermore, molecular dynamics simulations (MDS) were conducted for the most optimal complexes chosen based on their stability. Additionally, the absorption, distribution, metabolism, excretion, and toxicity (ADME-T) properties of novel pharmaceutical compounds have garnered increased interest in drug discovery [7]. Besides, the ADME-T and drug-likeness outcomes demonstrated the favorable pharmacokinetic proprieties and oral bioavailability of these substances. Consequently, the identified compounds are viable candidates for additional scrutiny and enhancement to craft novel lead compounds with enhanced efficacy against Philadelphia chromosome-positive ALL.

2. Materials and Methods

The 22 inhibitors used in our work are derivatives of phthalimido-1.3-thiazole. The optimization of the structures was carried out by molecular mechanics with the force field (MM+) implemented in the Hyperchem software [8]. Molecular docking and dynamic simulations of ligands and the crystal structure of human ABL1 kinase domain (PDB ID: 4WA9) were carried out using MOE 2014 (Molecular Operating Environment MOE) [9]. ADME-T prediction of the selected best compounds was conducted using some wed tool such as SwissADME (http://www.swissadme.ch/), and PKCSM (https://biosig.lab.uq.edu.au/pkcsm/).

3. Results

3.1. Molecular Docking

A molecular docking study was conducted for the twenty-two phthalimido-1,3-thiazole derivatives with the human ABL1 kinase domain in the 4WA9 protein PDB structure.

The total score energy results of the docked complexes with their distances, types of interactions, key residues, and atoms involved in the compounds and the receptor for the 4WA9 target, are summarized in Table 1, in this study the doxorubicin was taken as a reference.

Doxorubicin has score energy of −7.75 kcal/mol with the formation of two H-acceptor and Pi-H type interactions.

The six best compounds are ordered according to their affinity for the formation of stable complexes with the 4WA9 enzyme as follows: L21 > L20 > L22 > L19 > L17 > L18 with energy scores −9.29, −9.15, −9.02, −8.54, −8.41 and −8.36 (kcal/mol) respectively.

L21 gives the best energy score compared to the other compounds (−9.29 kcal/mol), Figure 1 indicates the 2D and 3D interaction diagrams between the active site of 4WA9 and L21.

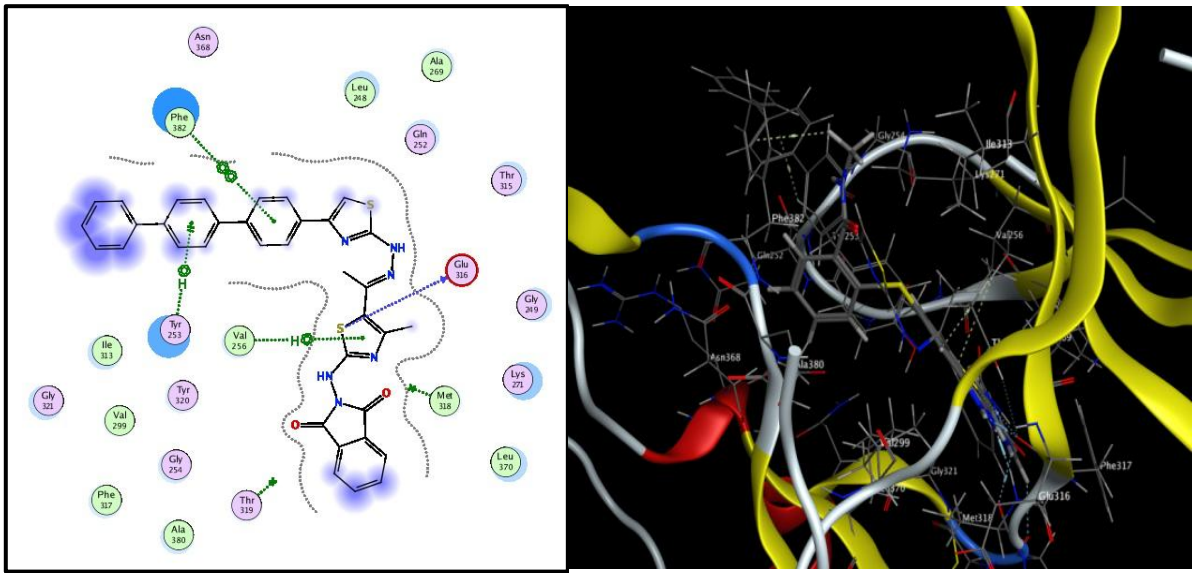

Figure 1. 2D and 3D interactions illustration of 4WA9-active site and L21.

Table 1. Docking score and interactions between compounds and active site amino acid residues of target 4WA9.

Complex	E Score kcal/mol	RMSD	Bonds Between Compound Atoms and Active Site Residues					
			Compound Atom	The Atoms Involved at the Receptor	Residues Involved at the Receptor	Type of Interactions	Distance (Å)	E (kcal/mol)
Doxo [1]	−7.7475	1.7921	O 23	N	GLY 254 [A]	H-acceptor	3.04	−1.8
			6-ring	CG2	ILE 313 [A]	Pi-H	4.49	−0.5
L17	−8.4152	2.8512	S 31	O	GLU 316 [A]	H-donor	3,94	− 0.9
			5-ring	6-ring	PHE382 [A]	Pi-Pi	3.60	− 0,0
L18	−8,3629	2.0503	N 26	6-ring	GLU 316 [A]	H-donor	2.93	−0.6
			5-ring	CB	ASP 381 [A]	Pi-H	3.74	−0.6
L19	−8,5473	1.3127	5-ring	CD	LYS 271 [A]	Pi-H	3.84	−0.5
			5-ring	CB	PHE 382 [A]	Pi-H	3.78	−0.7
L20	−9.1532	1.7784	6-ring	CA	LGL250 [A]	Pi-H	4.30	−0.5
			5-Ring	6-ring	PHE 382 [A]	Pi-H	3.61	−0,0
L21	−9.2920	2.5193	S 3	O	GLU 316 [A]	H-Donor	3.93	−1.0
			6-ring	CA	TRY 253 [A]	Pi-H	3.81	−1.0
			5-ring	CG2	VAL 256 [A]	Pi-H	4.42	−0.5
			6-ring	PHE	PHR 382 [A]	Pi-Pi	3.92	−0.0
L22	−9.0292	1.9701	5-ring	CD	LYS 271 [A]	Pi-H	4,15	−0,6
			N 22	6-ring	TRY 253 [A]	H-Pi	3.91	−1.5
			5-ring	CG2	VAL 256 [A]	Pi-H	4.36	−0.5
			6-ring	CD2	LEU 301 [A]	Pi-H	4.52	−0.5
			5-ring	CB	PHE382 [A]	Pi-H	4.15	−0.5

[1] Doxorubicin medication as a reference.

3.2. Molecular Dynamic Simulation

3.2.1. Ligand-Active Site Interactions

The complexes obtained from molecular docking are used as input in the simulation process for time intervals of 600 Ps each, and the potential energy value was collected every 0.5 ps. The results obtained are represented by curves of the potential energy U (kcal/mol) as a function of the simulation time (Ps) for the 4WA9-ligands complexes (Table 2).

In the 4WA9-L17 complex, the L17 ligand forms a weak bond with the 4WA9 receptor Pi-H type with the GLY 321 residue (3.49 A°).

The 4WA9-L18 complex presents three H-donor bonds: two strong bonds with THR 315 and GLY 250 of lengths 2.76 Å and 2.51 Å; a weak bond with residue GLU 316 of length 3.60 Å. We also notice a formation of two other weak H-acceptor bonds with GLY 321 and ASN 322 of length 3.44 Å. 3.23 Å. We also note the formation of a strong H-acceptor bond with ASN 322 distance (2.68 A°).

The 4WA9-L19 complex has two H-donor bonds with ASP 381 and MET 318 (2.66 A°, 3.38 A°) and two H-acceptor bonds with THR 315 and TYR 253 (2,75 A° and 3,00A°).

The 4WA9-L20 complex represents several interactions: two H-donor bonds with THR 315 (2.82 A°, 3.55 A°) and two strong H-acceptor type bonds with NME 272, TYR 253 (2.73 A°, 2.64A°).

In the 4WA9-L21 complex, we notice the formation of three weak Pi-H type interactions with LEU 301, ASN 322 (4.31 A° 4.00 A° 3.97 A°) and a weak H-donor bond with THR 315 (4.05 A°).

The 4WA9-L22 complex presents two weak Pi-H type interactions with LYS 271 and GLY 321, (3.90 A°, 3.97 A°).

Table 2. different interactions result from MD simulation.

Complexe	Bonds Between Compound Atoms and Active Site Residues					
	Compound Atom	**The Atoms Involved at the Receptor**	**Residues Involved at the Receptor**	**Type of Interactions**	**Distance (Å)**	**E (Kcal/mol)**
4wa9-L 17	5-ring	CA	GLY 321	Pi-H	3.49	−0.8
4wa9-L 18	N 25	OG1	THR 315	H-donor	2.76	−2.7
	S 35	O	GLU 316	H-donor	3.60	−0.7
	N 50	O	GLY 250	H-donor	2.51	−3.8
	O 52	CA	GLY 321	H-acceptor	3.44	−0.9
	O 52	N	ASN 322	H-acceptor	3.23	−1.9
	O 52	ND2	ASN 322	H-acceptor	2.68	−6.6
4wa9-L 19	N 15	OD1	ASP 381	H-donor	2.66	−7.8
	C 36	O	MET 318	H-donor	3.38	−0.8
	O 13	OG1	THR 315	H-acceptor	2.75	−2.0
	N 37	OH	TYR 253	H-acceptor	3.00	−1.0
4wa9-L 20	N 15	OG1	THR 315	H-donor	2.82	−4.0
	S 21	OG1	THR 315	H-donor	3.55	−1.3
	O 14	N	NME 272	H-acceptor	2.73	−3.0
	N 37	OH	TYR 253	H-acceptor	2.64	−2.2
	6-ring	CD1	LEU 248	Pi-H	4.52	−0.6
	5-ring	CG1	VAL 256	Pi-H	4.65	−0.6
	6-ring	CA	GLY 321	Pi-H	4.49	−1.1
4wa9-L 21	S 5	OG1	THR 315	H-donor	4.05	−0.6
	5-ring	CD1	LEU 301	Pi-H	4.31	−0.6
	6-ring	CB	ASN 322	Pi-H	4.00	−1.2
	6-ring	ND2	ASN 322	Pi-H	3.97	−0.8
4wa9-L 22	5-ring	CG	LYS 271	Pi-H	3.90	−1.2
	6-ring	CA	GLY 321	Pi-H	3.97	−0.9

3.2.2. Potential Energy During Simulation Time

The variation of the potential energy during time of complexes 4WA9-L17, 4WA9-L18.4WA9-L19, 4WA9-L20, 4WA9-L21, and 4WA9-L22 is shown in Figure 2.

The 4WA9-L17 complex has a potential energy variation of −75.12 at 2392 kcal/mol during the first 100 Pico seconds.

We also note a variation in potential energy: 2400 to 2342 kcal/mol in the second part of the interval between 100 and 350 picoseconds, and finally, in the last interval between 350 and 600 picoseconds, we have an energy variation potential from 2290 to 2218 kcal/mol.

But in the 4WA9-L18 complex, the potential energy is -169.91 to 2373 kcal/mol during the first 100 picoseconds. In the second part of the interval between 100 and 350 picoseconds, there is a variation of the potential energy from 2373 to 2325 kcal/mol and finally, in 350 and 600 Picosecond we have a potential energy variation from 2325 to 2293 kcal/mol.

The 4WA9-L19 complex has a potential energy varying from −222 to 2371 kcal/mol during the first 100 picoseconds. Between 100 and 350 picoseconds, a potential energy varied from 2371 to 2315 kcal/mol. In the last interval between 350 and 600 Picosecond, the potential energy varies from 2315 to 2351 kcal/mol.

The potential energy of the 4WA9-L20 complex varies from −206 to 2475 kcal/mol in the first 100 picoseconds, and varied from 2475 to 2348 kcal/mol in the second part of the interval between 100 and 350 picoseconds. In the last interval between 350 and 600 picoseconds the potential energy varies from 2336 to 2359 kcal/mol.

The 4WA9-L21 complex having a potential energy varies from −95 to 2438 kcal/mol during the first 100 picoseconds, and varies from 2438 to 2291 kcal/mol in the second part of the interval between 100 and 350 picoseconds. Finally, in the last interval between 350 and 600 picoseconds the potential energy varies from 2291 to 2269 kcal/mol.

The potential energy of the 4WA9-L22 complex varies from −67 to 2478 kcal/mol in the domain (0–100 Ps), varies from 2478 to 2233 kcal/mol in the interval between (100–350 Ps), finally, varies from 2233 to 2210 kcal/mol in the interval 350–600 picosecond.

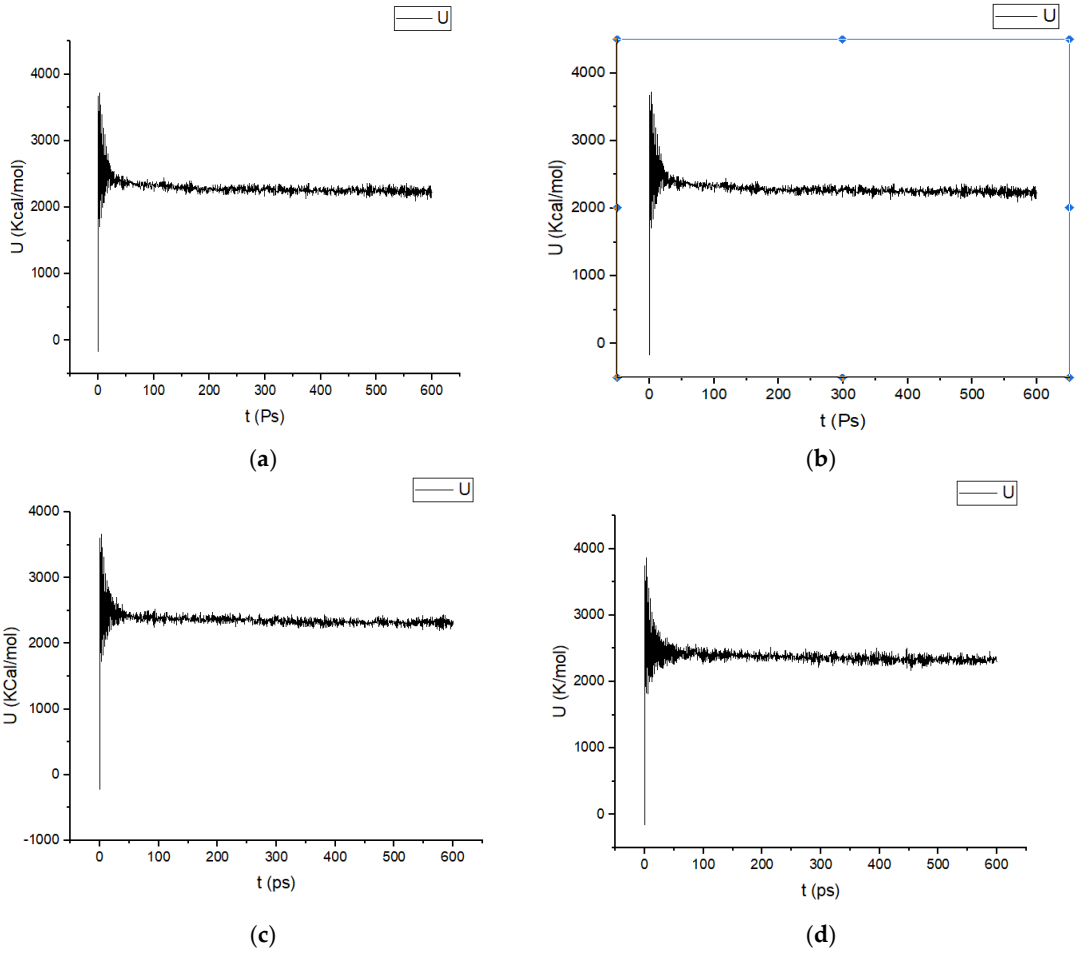

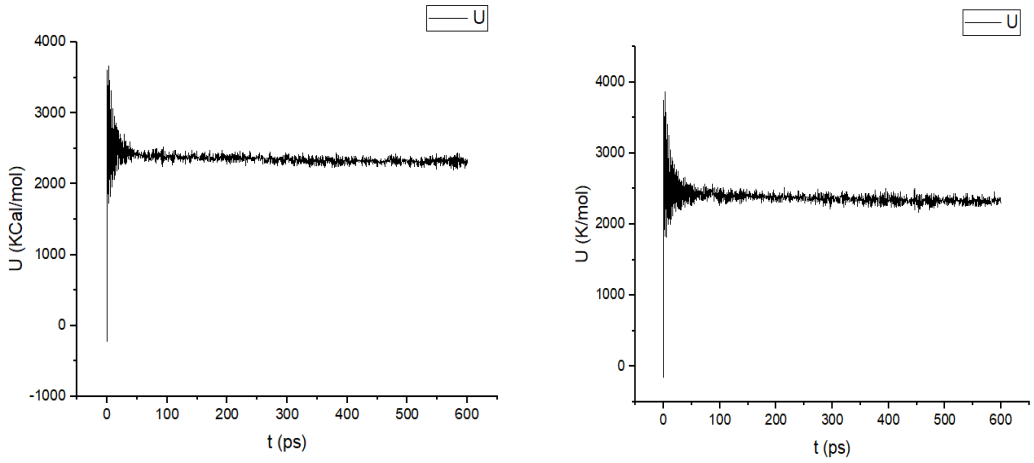

(**e**) (**f**)

Figure 2. Potential energy U (kcal/mol) variations as a function of time of the studied complexes (**a**) U of 4WA9-L17, (**b**) U of 4WA9-L18, (**c**) U of 4WA9-L19, (**d**) U of 4WA9-L20, (**e**) U of 4WA9-L121, (**f**) U of 4WA9 -L22.

Author Contributions: Data collection, software, formal analysis, and the first draft of the manuscript were prepared by I.B. and A.F. All authors commented on previous versions of the manuscript. N.M. contributed to the conceptualization, project administration, and supervision. I.D. guaranteed the validation and data curation of this study. All authors have read and agreed to the published version of the manuscript.

Funding: Please add: This research received no external funding.

Informed Consent Statement: Informed consent was obtained from all subjects involved in the study.

Data Availability Statement: Not applicable.

Conflicts of Interest: The authors declare that they have no conflict of interest.

References

1. Axitinib Effectively Inhibits BCR-ABL1 (T315I) with a Distinct Binding Conformation. Nature. Available online: https://www.nature.com/articles/nature14119 (accessed on 21 June 2024).
2. Peppas, I.; Ford, A.M.; Furness, C.L.; Greaves, M.F. Gut microbiome immaturity and childhood acute lymphoblastic leukaemia. *Nat. Rev. Cancer* **2023**, *23*, 565–576. https://doi.org/10.1038/s41568-023-00584-4.
3. Philadelphia Chromosome-Positive Leukemia in the Lymphoid Lineage—Similarities and Differences with the Myeloid Lineage and Specific Vulnerabilities—PMC. Available online: https://www.ncbi.nlm.nih.gov/pmc/articles/PMC7460962/ (accessed on 21 June 2024).
4. Cario, G.; Leoni, V.; Conter, V.; Baruchel, A.; Schrappe, M.; Biondi, A. BCR-ABL1-like acute lymphoblastic leukemia in childhood and targeted therapy. *Haematologica* **2020**, *105*, 2200–2204. https://doi.org/10.3324/haematol.2018.207019.
5. Oliveira, A.R.; Dos Santos, F.A.; Ferreira, L.P.d.L.; Pitta, M.G.d.R.; Silva, M.V.d.O.; Cardoso, M.V.d.O.; Pinto, A.F.; Marchand, P.; de Melo Rêgo, M.J.B.; Leite, A.C.L. Synthesis, anticancer activity and mechanism of action of new phthalimido-1,3-thiazole derivatives. *Chem. Biol. Interact.* **2021**, *347*, 109597. https://doi.org/10.1016/j.cbi.2021.109597.
6. Saghiri, K.; Daoud, I.; Melkemi, N.; Mesli, F. Molecular docking/dynamics simulations, MEP analysis, and pharmacokinetics prediction of some withangulatin A derivatives as allosteric glutaminase C inhibitors in breast cancer. *Chem. Data Collect.* **2023**, *46*, 101044. https://doi.org/10.1016/j.cdc.2023.101044.
7. Mettai, M.; Daoud, I.; Mesli, F.; Kenouche, S.; Melkemi, N.; Kherachi, R.; Belkadi, A. Molecular docking/dynamics simulations, MEP analysis, bioisosteric replacement and ADME/T prediction for identification of dual targets inhibitors of Parkinson's disease with novel scaffold. *In Silico Pharmacol.* **2023**, *11*, 3. https://doi.org/10.1007/s40203-023-00139-3.
8. *HyperChem(TM) Professional 7.51*; Hypercube, Inc.: Gainesville, FL, USA.

9. Molecular Operating Environment (MOE) 2014. Chemical Computing Group Inc.: Montreal, Quebec, Canada, 2014. Available online: https://www.chemcomp.com/ (accessed on).
10. Durán-Iturbide, N.A.; Díaz-Eufracio, B.I.; Medina-Franco, J.L. In Silico ADME/Tox Profiling of Natural Products: A Focus on BIOFACQUIM. *ACS Omega* **2020**, *5*, 16076–16084.